PHYSICAL REVIEW D **85,** 082002 (2012)

Search for gravitational waves from low mass compact binary coalescence in LIGO's sixth science run and Virgo's science runs 2 and 3

J. Abadie,[1,a] B. P. Abbott,[1,a] R. Abbott,[1,a] T. D. Abbott,[2,a] M. Abernathy,[3,a] T. Accadia,[4,b] F. Acernese,[5a,5c,b] C. Adams,[6,a] R. Adhikari,[1,a] C. Affeldt,[7,8,a] M. Agathos,[9a,b] P. Ajith,[1,a] B. Allen,[7,10,8,a] G. S. Allen,[11,a] E. Amador Ceron,[10,a] D. Amariutei,[12,a] R. S. Amin,[13,a] S. B. Anderson,[1,a] W. G. Anderson,[10,a] K. Arai,[1,a] M. A. Arain,[12,a] M. C. Araya,[1,a] S. M. Aston,[14,a] P. Astone,[15a,b] D. Atkinson,[16,a] P. Aufmuth,[8,7,a] C. Aulbert,[7,8,a] B. E. Aylott,[14,a] S. Babak,[17,a] P. Baker,[18,a] G. Ballardin,[19,b] S. Ballmer,[20,a] D. Barker,[16,a] F. Barone,[5a,5c,b] B. Barr,[3,a] P. Barriga,[21,a] L. Barsotti,[22,a] M. Barsuglia,[23,b] M. A. Barton,[16,a] I. Bartos,[24,a] R. Bassiri,[3,a] M. Bastarrika,[3,a] A. Basti,[25a,25b,b] J. Batch,[16,a] J. Bauchrowitz,[7,8,a] Th. S. Bauer,[9a,b] M. Bebronne,[4,b] B. Behnke,[17,a] M. G. Beker,[9a,b] A. S. Bell,[3,a] A. Belletoile,[4,b] I. Belopolski,[24,a] M. Benacquista,[26,a] J. M. Berliner,[16,a] A. Bertolini,[7,8,a] J. Betzwieser,[1,a] N. Beveridge,[3,a] P. T. Beyersdorf,[27,a] I. A. Bilenko,[28,a] G. Billingsley,[1,a] J. Birch,[6,a] R. Biswas,[26,a] M. Bitossi,[25a,b] M. A. Bizouard,[29a,b] E. Black,[1,a] J. K. Blackburn,[1,a] L. Blackburn,[30,a] D. Blair,[21,a] B. Bland,[16,a] M. Blom,[9a,b] O. Bock,[7,8,a] T. P. Bodiya,[22,a] C. Bogan,[7,8,a] R. Bondarescu,[31,a] F. Bondu,[32b,b] L. Bonelli,[25a,25b,b] R. Bonnand,[33,b] R. Bork,[1,a] M. Born,[7,8,a] V. Boschi,[25a,b] S. Bose,[34,a] L. Bosi,[35a,b] B. Bouhou,[23,b] S. Braccini,[25a,b] C. Bradaschia,[25a,b] P. R. Brady,[10,a] V. B. Braginsky,[28,a] M. Branchesi,[36a,36b,b] J. E. Brau,[37,a] J. Breyer,[7,8,a] T. Briant,[38,b] D. O. Bridges,[6,a] A. Brillet,[32a,b] M. Brinkmann,[7,8,a] V. Brisson,[29a,b] M. Britzger,[7,8,a] A. F. Brooks,[1,a] D. A. Brown,[20,a] A. Brummit,[39,a] T. Bulik,[40b,40c,b] H. J. Bulten,[9a,9b,b] A. Buonanno,[41,a] J. Burguet–Castell,[10,a] O. Burmeister,[7,8,a] D. Buskulic,[4,b] C. Buy,[23,b] R. L. Byer,[11,a] L. Cadonati,[42,a] G. Cagnoli,[36a,b] E. Calloni,[5a,5b,b] J. B. Camp,[30,a] P. Campsie,[3,a] J. Cannizzo,[30,a] K. Cannon,[43,a] B. Canuel,[19,b] J. Cao,[44,a] C. D. Capano,[20,a] F. Carbognani,[19,b] S. Caride,[45,a] S. Caudill,[13,a] M. Cavaglià,[46,a] F. Cavalier,[29a,b] R. Cavalieri,[19,b] G. Cella,[25a,b] C. Cepeda,[1,a] E. Cesarini,[36b,b] O. Chaibi,[32a,b] T. Chalermsongsak,[1,a] E. Chalkley,[14,a] P. Charlton,[47,a] E. Chassande-Mottin,[23,b] S. Chelkowski,[14,a] Y. Chen,[48,a] A. Chincarini,[49,b] A. Chiummo,[19,b] H. Cho,[50,a] N. Christensen,[51,a] S. S. Y. Chua,[52,a] C. T. Y. Chung,[53,a] S. Chung,[21,a] G. Ciani,[12,a] F. Clara,[16,a] D. E. Clark,[11,a] J. Clark,[54,a] J. H. Clayton,[10,a] F. Cleva,[32a,b] E. Coccia,[55a,55b,b] P.-F. Cohadon,[38,b] C. N. Colacino,[25a,25b,b] J. Colas,[19,b] A. Colla,[15a,15b,b] M. Colombini,[15b,b] A. Conte,[15a,15b,b] R. Conte,[56,a] D. Cook,[16,a] T. R. Corbitt,[22,a] M. Cordier,[27,a] N. Cornish,[18,a] A. Corsi,[1,a] C. A. Costa,[13,a] M. Coughlin,[51,a] J.-P. Coulon,[32a,b] P. Couvares,[20,a] D. M. Coward,[21,a] D. C. Coyne,[1,a] J. D. E. Creighton,[10,a] T. D. Creighton,[26,a] A. M. Cruise,[14,a] A. Cumming,[3,a] L. Cunningham,[3,a] E. Cuoco,[19,b] R. M. Cutler,[14,a] K. Dahl,[7,8,a] S. L. Danilishin,[28,a] R. Dannenberg,[1,a] S. D'Antonio,[55a,b] K. Danzmann,[7,8,a] V. Dattilo,[19,b] B. Daudert,[1,a] H. Daveloza,[26,a] M. Davier,[29a,b] G. Davies,[54,a] E. J. Daw,[57,a] R. Day,[19,b] T. Dayanga,[34,a] R. De Rosa,[5a,5b,b] D. DeBra,[11,a] G. Debreczeni,[58,a] J. Degallaix,[7,8,a] W. Del Pozzo,[9a,b] M. del Prete,[59b,b] T. Dent,[54,a] V. Dergachev,[1,a] R. DeRosa,[13,a] R. DeSalvo,[1,a] S. Dhurandhar,[60,a] L. Di Fiore,[5a,b] A. Di Lieto,[25a,25b,b] I. Di Palma,[7,8,a] M. Di Paolo Emilio,[55a,55c,b] A. Di Virgilio,[25a,b] M. Díaz,[26,a] A. Dietz,[4,b] J. DiGuglielmo,[7,8,a] F. Donovan,[22,a] K. L. Dooley,[12,a] S. Dorsher,[61,a] M. Drago,[59a,59b,b] R. W. P. Drever,[62,a] J. C. Driggers,[1,a] Z. Du,[44,a] J.-C. Dumas,[21,a] S. Dwyer,[22,a] T. Eberle,[7,8,a] M. Edgar,[3,a] M. Edwards,[54,a] A. Effler,[13,a] P. Ehrens,[1,a] G. Endrőczi,[58,a] R. Engel,[1,a] T. Etzel,[1,a] K. Evans,[3,a] M. Evans,[22,a] T. Evans,[6,a] M. Factourovich,[24,a] V. Fafone,[55a,55b,b] S. Fairhurst,[54,a] Y. Fan,[21,a] B. F. Farr,[63,a] W. Farr,[63,a] D. Fazi,[63,a] H. Fehrmann,[7,8,a] D. Feldbaum,[12,a] I. Ferrante,[25a,25b,b] F. Fidecaro,[25a,25b,b] L. S. Finn,[31,a] I. Fiori,[19,b] R. P. Fisher,[31,a] R. Flaminio,[33,b] M. Flanigan,[16,a] S. Foley,[22,a] E. Forsi,[6,a] L. A. Forte,[5a,b] N. Fotopoulos,[1,a] J.-D. Fournier,[32a,b] J. Franc,[33,b] S. Frasca,[15a,15b,b] F. Frasconi,[25a,b] M. Frede,[7,8,a] M. Frei,[64,a] Z. Frei,[65,a] A. Freise,[14,a] R. Frey,[37,a] T. T. Fricke,[13,a] D. Friedrich,[7,8,a] P. Fritschel,[22,a] V. V. Frolov,[6,a] P. J. Fulda,[14,a] M. Fyffe,[6,a] M. Galimberti,[33,b] L. Gammaitoni,[35a,35b,b] M. R. Ganija,[66,a] J. Garcia,[16,a] J. A. Garofoli,[20,a] F. Garufi,[5a,5b,b] M. E. Gáspár,[58,a] G. Gemme,[49,b] R. Geng,[44,a] E. Genin,[19,b] A. Gennai,[25a,b] L. Á. Gergely,[67,a] S. Ghosh,[34,a] J. A. Giaime,[13,6,a] S. Giampanis,[10,a] K. D. Giardina,[6,a] A. Giazotto,[25a,b] C. Gill,[3,a] E. Goetz,[7,8,a] L. M. Goggin,[10,a] G. González,[13,a] M. L. Gorodetsky,[28,a] S. Goßler,[7,8,a] R. Gouaty,[4,b] C. Graef,[7,8,a] M. Granata,[23,b] A. Grant,[3,a] S. Gras,[21,a] C. Gray,[16,a] N. Gray,[3,a] R. J. S. Greenhalgh,[39,a] A. M. Gretarsson,[68,a] C. Greverie,[32a,b] R. Grosso,[26,a] H. Grote,[7,8,a] S. Grunewald,[17,a] G. M. Guidi,[36a,36b,b] C. Guido,[6,a] R. Gupta,[60,a] E. K. Gustafson,[1,a] R. Gustafson,[45,a] T. Ha,[69,a] B. Hage,[8,7,a] J. M. Hallam,[14,a] D. Hammer,[10,a] G. Hammond,[3,a] J. Hanks,[16,a] C. Hanna,[1,70,a] J. Hanson,[6,a] A. Hardt,[51,a] J. Harms,[62,a] G. M. Harry,[22,a] I. W. Harry,[54,a] E. D. Harstad,[37,a] M. T. Hartman,[12,a] K. Haughian,[3,a] K. Hayama,[71,a] J.-F. Hayau,[32b,b] J. Heefner,[1,a] A. Heidmann,[38,b] M. C. Heintze,[12,a] H. Heitmann,[32a,a] P. Hello,[29a,b] M. A. Hendry,[3,a] I. S. Heng,[3,a] A. W. Heptonstall,[1,a] V. Herrera,[11,a] M. Hewitson,[7,8,a] S. Hild,[3,a] D. Hoak,[42,a] K. A. Hodge,[1,a] K. Holt,[6,a] T. Hong,[48,a] S. Hooper,[21,a] D. J. Hosken,[66,a] J. Hough,[3,a] E. J. Howell,[21,a] B. Hughey,[10,a] S. Husa,[72,a] S. H. Huttner,[3,a] T. Huynh-Dinh,[6,a] D. R. Ingram,[16,a] R. Inta,[52,a] T. Isogai,[51,a] A. Ivanov,[1,a] K. Izumi,[71,a] M. Jacobson,[1,a] H. Jang,[73,a] P. Jaranowski,[40d,b] W. W. Johnson,[13,a] D. I. Jones,[74,a] G. Jones,[54,a] R. Jones,[3,a] L. Ju,[21,a]

P. Kalmus,[1,a] V. Kalogera,[63,a] I. Kamaretsos,[54,a] S. Kandhasamy,[61,a] G. Kang,[73,a] J. B. Kanner,[41,a] E. Katsavounidis,[22,a] W. Katzman,[6,a] H. Kaufer,[7,8,a] K. Kawabe,[16,a] S. Kawamura,[71,a] F. Kawazoe,[7,8,a] W. Kells,[1,a] D. G. Keppel,[1,a] Z. Keresztes,[67,a] A. Khalaidovski,[7,8,a] F. Y. Khalili,[28,a] E. A. Khazanov,[75,a] B. Kim,[73,a] C. Kim,[76,a] D. Kim,[21,a] H. Kim,[7,8,a] K. Kim,[77,a] N. Kim,[11,a] Y.-M. Kim,[50,a] P. J. King,[1,a] M. Kinsey,[31,a] D. L. Kinzel,[6,a] J. S. Kissel,[22,a] S. Klimenko,[12,a] K. Kokeyama,[14,a] V. Kondrashov,[1,a] R. Kopparapu,[31,a] S. Koranda,[10,a] W. Z. Korth,[1,a] I. Kowalska,[40b,b] D. Kozak,[1,a] V. Kringel,[7,8,a] S. Krishnamurthy,[63,a] B. Krishnan,[17,a] A. Królak,[40a,40e,b] G. Kuehn,[7,8,a] R. Kumar,[3,a] P. Kwee,[8,7,a] P. K. Lam,[52,a] M. Landry,[16,a] M. Lang,[31,a] B. Lantz,[11,a] N. Lastzka,[7,8,a] C. Lawrie,[3,a] A. Lazzarini,[1,a] P. Leaci,[17,a] C. H. Lee,[50,a] H. M. Lee,[78,a] N. Leindecker,[11,a] J. R. Leong,[7,8,a] I. Leonor,[37,a] N. Leroy,[29a,b] N. Letendre,[4,b] J. Li,[44,a] T. G. F. Li,[9a,b] N. Liguori,[59a,59b,b] P. E. Lindquist,[1,a] N. A. Lockerbie,[79,a] D. Lodhia,[14,a] M. Lorenzini,[36a,b] V. Loriette,[29b,b] M. Lormand,[6,a] G. Losurdo,[36a,b] J. Luan,[48,a] M. Lubinski,[16,a] H. Lück,[7,8,a] A. P. Lundgren,[31,a] E. Macdonald,[3,a] B. Machenschalk,[7,8,a] M. MacInnis,[22,a] D. M. Macleod,[54,a] M. Mageswaran,[1,a] K. Mailand,[1,a] E. Majorana,[15a,b] I. Maksimovic,[29b,b] N. Man,[32a,b] I. Mandel,[22,a] V. Mandic,[61,a] M. Mantovani,[25a,25c,b] A. Marandi,[11,a] F. Marchesoni,[35a,b] F. Marion,[4,b] S. Márka,[24,a] Z. Márka,[24,a] A. Markosyan,[11,a] E. Maros,[1,a] J. Marque,[19,b] F. Martelli,[36a,36b,b] I. W. Martin,[3,a] R. M. Martin,[12,a] J. N. Marx,[1,a] K. Mason,[22,a] A. Masserot,[4,b] F. Matichard,[22,a] L. Matone,[24,a] R. A. Matzner,[64,a] N. Mavalvala,[22,a] G. Mazzolo,[7,8,a] R. McCarthy,[16,a] D. E. McClelland,[52,a] S. C. McGuire,[80,a] G. McIntyre,[1,a] J. McIver,[42,a] D. J. A. McKechan,[54,a] G. D. Meadors,[45,a] M. Mehmet,[7,8,a] T. Meier,[8,7,a] A. Melatos,[53,a] A. C. Melissinos,[81,a] G. Mendell,[16,a] D. Menendez,[31,a] R. A. Mercer,[10,a] S. Meshkov,[1,a] C. Messenger,[54,a] M. S. Meyer,[6,a] H. Miao,[21,a] C. Michel,[33,b] L. Milano,[5a,5b,b] J. Miller,[52,a] Y. Minenkov,[55a,b] V. P. Mitrofanov,[28,a] G. Mitselmakher,[12,a] R. Mittleman,[22,a] O. Miyakawa,[71,a] B. Moe,[10,a] P. Moesta,[17,a] M. Mohan,[19,b] S. D. Mohanty,[26,a] S. R. P. Mohapatra,[42,a] D. Moraru,[16,a] G. Moreno,[16,a] N. Morgado,[33,b] A. Morgia,[55a,55b,b] T. Mori,[71,a] S. Mosca,[5a,5b,b] K. Mossavi,[7,8,a] B. Mours,[4,b] C. M. Mow-Lowry,[52,a] C. L. Mueller,[12,a] G. Mueller,[12,a] S. Mukherjee,[26,a] A. Mullavey,[52,a] H. Müller-Ebhardt,[7,8,a] J. Munch,[66,a] D. Murphy,[24,a] P. G. Murray,[3,a] A. Mytidis,[12,a] T. Nash,[1,a] L. Naticchioni,[15a,15b,b] R. Nawrodt,[3,a] V. Necula,[12,a] J. Nelson,[3,a] G. Newton,[3,a] A. Nishizawa,[71,a] F. Nocera,[19,b] D. Nolting,[6,a] L. Nuttall,[54,a] E. Ochsner,[41,a] J. O'Dell,[39,a] E. Oelker,[22,a] G. H. Ogin,[1,a] J. J. Oh,[69,a] S. H. Oh,[69,a] R. G. Oldenburg,[10,a] B. O'Reilly,[6,a] R. O'Shaughnessy,[10,a] C. Osthelder,[1,a] C. D. Ott,[48,a] D. J. Ottaway,[66,a] R. S. Ottens,[12,a] H. Overmier,[6,a] B. J. Owen,[31,a] A. Page,[14,a] G. Pagliaroli,[55a,55c,b] L. Palladino,[55a,55c,b] C. Palomba,[15a,b] Y. Pan,[41,a] C. Pankow,[12,a] F. Paoletti,[25a,19,b] M. A. Papa,[17,10,a] M. Parisi,[5a,5b,b] A. Pasqualetti,[19,b] R. Passaquieti,[25a,25b,b] D. Passuello,[25a,b] P. Patel,[1,a] M. Pedraza,[1,a] P. Peiris,[82,a] L. Pekowsky,[20,a] S. Penn,[83,a] C. Peralta,[17,a] A. Perreca,[20,a] G. Persichetti,[5a,5b,b] M. Phelps,[1,a] M. Pickenpack,[7,8,a] F. Piergiovanni,[36a,36b,b] M. Pietka,[40d,b] L. Pinard,[33,b] I. M. Pinto,[84,a] M. Pitkin,[3,a] H. J. Pletsch,[7,8,a] M. V. Plissi,[3,a] R. Poggiani,[25a,25b,b] J. Pöld,[7,8,a] F. Postiglione,[56,a] M. Prato,[49,b] V. Predoi,[54,a] L. R. Price,[1,a] M. Prijatelj,[7,8,a] M. Principe,[84,a] S. Privitera,[1,a] R. Prix,[7,8,a] G. A. Prodi,[59a,59b,b] L. Prokhorov,[28,a] O. Puncken,[7,8,a] M. Punturo,[35a,b] P. Puppo,[15a,b] V. Quetschke,[26,a] F. J. Raab,[16,a] D. S. Rabeling,[9a,9b,b] I. Rácz,[58,a] H. Radkins,[16,a] P. Raffai,[65,a] M. Rakhmanov,[26,a] C. R. Ramet,[6,a] B. Rankins,[46,a] P. Rapagnani,[15a,15b,b] V. Raymond,[63,a] V. Re,[55a,55b,b] K. Redwine,[24,a] C. M. Reed,[16,a] T. Reed,[85,a] T. Regimbau,[32a,b] S. Reid,[3,a] D. H. Reitze,[12,a] F. Ricci,[15a,15b,b] R. Riesen,[6,a] K. Riles,[45,a] N. A. Robertson,[1,3,a] F. Robinet,[29a,b] C. Robinson,[54,a] E. L. Robinson,[17,a] A. Rocchi,[55a,b] S. Roddy,[6,a] C. Rodriguez,[63,a] M. Rodruck,[16,a] L. Rolland,[4,b] J. Rollins,[24,a] J. D. Romano,[26,a] R. Romano,[5a,5c,b] J. H. Romie,[6,a] D. Rosińska,[40c,40f,b] C. Röver,[7,8,a] S. Rowan,[3,a] A. Rüdiger,[7,8,a] P. Ruggi,[19,b] K. Ryan,[16,a] H. Ryll,[7,8,a] P. Sainathan,[12,a] M. Sakosky,[16,a] F. Salemi,[7,8,a] A. Samblowski,[7,8,a] L. Sammut,[53,a] L. Sancho de la Jordana,[72,a] V. Sandberg,[16,a] S. Sankar,[22,a] V. Sannibale,[1,a] L. Santamaría,[1,a] I. Santiago-Prieto,[3,a] G. Santostasi,[86,a] B. Sassolas,[33,b] B. S. Sathyaprakash,[54,a] S. Sato,[71,a] P. R. Saulson,[20,a] R. L. Savage,[16,a] R. Schilling,[7,8,a] S. Schlamminger,[87,a] R. Schnabel,[7,8,a] R. M. S. Schofield,[37,a] B. Schulz,[7,8,a] B. F. Schutz,[17,54,a] P. Schwinberg,[16,a] J. Scott,[3,a] S. M. Scott,[52,a] A. C. Searle,[1,a] F. Seifert,[1,a] D. Sellers,[6,a] A. S. Sengupta,[1,a] D. Sentenac,[19,b] A. Sergeev,[75,a] D. A. Shaddock,[52,a] M. Shaltev,[7,8,a] B. Shapiro,[22,a] P. Shawhan,[41,a] D. H. Shoemaker,[22,a] A. Sibley,[6,a] X. Siemens,[10,a] D. Sigg,[16,a] A. Singer,[1,a] L. Singer,[1,a] A. M. Sintes,[72,a] G. Skelton,[10,a] B. J. J. Slagmolen,[52,a] J. Slutsky,[13,a] J. R. Smith,[2,a] M. R. Smith,[1,a] N. D. Smith,[22,a] R. J. E. Smith,[14,a] K. Somiya,[48,a] B. Sorazu,[3,a] J. Soto,[22,a] F. C. Speirits,[3,a] L. Sperandio,[55a,55b,b] M. Stefszky,[52,a] A. J. Stein,[22,a] E. Steinert,[16,a] J. Steinlechner,[7,8,a] S. Steinlechner,[7,8,a] S. Steplewski,[34,a] A. Stochino,[1,a] R. Stone,[26,a] K. A. Strain,[3,a] S. Strigin,[28,a] A. S. Stroeer,[26,a] R. Sturani,[36a,36b,b] A. L. Stuver,[6,a] T. Z. Summerscales,[88,a] M. Sung,[13,a] S. Susmithan,[21,a] P. J. Sutton,[54,a] B. Swinkels,[19,b] M. Tacca,[19,b] L. Taffarello,[59c,b] D. Talukder,[34,a] D. B. Tanner,[12,a] S. P. Tarabrin,[7,8,a] J. R. Taylor,[7,8,a] R. Taylor,[1,a] P. Thomas,[16,a] K. A. Thorne,[6,a] K. S. Thorne,[48,a] E. Thrane,[61,a] A. Thüring,[8,7,a] C. Titsler,[31,a] K. V. Tokmakov,[79,a] A. Toncelli,[25a,25b,b] M. Tonelli,[25a,25b,b] O. Torre,[25a,25c,b] C. Torres,[6,a] C. I. Torrie,[1,3,a] E. Tournefier,[4,b] F. Travasso,[35a,35b,b] G. Traylor,[6,a] M. Trias,[72,a] K. Tseng,[11,a] E. Tucker,[51,a] D. Ugolini,[89,a] K. Urbanek,[11,a] H. Vahlbruch,[8,7,a]

G. Vajente,[25a,25b,b] M. Vallisneri,[48,a] J. F. J. van den Brand,[9a,9b,b] C. Van Den Broeck,[9a,b] S. van der Putten,[9a,b] A. A. van Veggel,[3,a] S. Vass,[1,a] M. Vasuth,[58,a] R. Vaulin,[22,a] M. Vavoulidis,[29a,b] A. Vecchio,[14,a] G. Vedovato,[59c,b] J. Veitch,[54,a] P. J. Veitch,[66,a] C. Veltkamp,[7,8,a] D. Verkindt,[4,b] F. Vetrano,[36a,36b,b] A. Viceré,[36a,36b,b] A. E. Villar,[1,a] J.-Y. Vinet,[32a,b] S. Vitale,[68,a] S. Vitale,[9a,b] H. Vocca,[35a,b] C. Vorvick,[16,a] S. P. Vyatchanin,[28,a] A. Wade,[52,a] S. J. Waldman,[22,a] L. Wallace,[1,a] Y. Wan,[44,a] X. Wang,[44,a] Z. Wang,[44,a] A. Wanner,[7,8,a] R. L. Ward,[23,b] M. Was,[29a,b] P. Wei,[20,a] M. Weinert,[7,8,a] A. J. Weinstein,[1,a] R. Weiss,[22,a] L. Wen,[48,21,a] S. Wen,[6,a] P. Wessels,[7,8,a] M. West,[20,a] T. Westphal,[7,8,a] K. Wette,[7,8,a] J. T. Whelan,[82,a] S. E. Whitcomb,[1,21,a] D. White,[57,a] B. F. Whiting,[12,a] C. Wilkinson,[16,a] P. A. Willems,[1,a] H. R. Williams,[31,a] L. Williams,[12,a] B. Willke,[7,8,a] L. Winkelmann,[7,8,a] W. Winkler,[7,8,a] C. C. Wipf,[22,a] A. G. Wiseman,[10,a] H. Wittel,[7,8,a] G. Woan,[3,a] R. Wooley,[6,a] J. Worden,[16,a] J. Yablon,[63,a] I. Yakushin,[6,a] H. Yamamoto,[1,a] K. Yamamoto,[7,8,a] H. Yang,[48,a] D. Yeaton-Massey,[1,a] S. Yoshida,[90,a] P. Yu,[10,a] M. Yvert,[4,b] A. Zadrożny,[40e,b] M. Zanolin,[68,a] J.-P. Zendri,[59c,b] F. Zhang,[44,a] L. Zhang,[1,a] W. Zhang,[44,a] Z. Zhang,[21,a] C. Zhao,[21,a] N. Zotov,[85,a] M. E. Zucker,[22,a] and J. Zweizig[1,a]

([a]LIGO Scientific Collaboration)
([b]Virgo Collaboration)

[1]*LIGO-California Institute of Technology, Pasadena, California 91125, USA*
[2]*California State University Fullerton, Fullerton California 92831 USA*
[3]*SUPA, University of Glasgow, Glasgow, G12 8QQ, United Kingdom*
[4]*Laboratoire d'Annecy-le-Vieux de Physique des Particules (LAPP), , USAUniversité de Savoie, CNRS/IN2P3, F-74941 Annecy-Le-Vieux, France*
[5a]*INFN, Sezione di Napoli, Italy*
[5b]*Università di Napoli 'Federico II' Complesso Universitario di Monte S.Angelo, I-80126 Napoli, Italy*
[5c]*Università di Salerno, Fisciano, I-84084 Salerno, Italy*
[6]*LIGO-Livingston Observatory, Livingston, Louisiana 70754, USA*
[7]*Albert-Einstein-Institut, Max-Planck-Institut für Gravitationsphysik, D-30167 Hannover, Germany*
[8]*Leibniz Universität Hannover, D-30167 Hannover, Germany*
[9a]*Nikhef, Science Park, Amsterdam, the Netherlands*
[9b]*VU University Amsterdam, De Boelelaan 1081, 1081 HV Amsterdam, the Netherlands*
[10]*University of Wisconsin-Milwaukee, Milwaukee, Wisconsin 53201, USA*
[11]*Stanford University, Stanford, California 94305, USA*
[12]*University of Florida, Gainesville, Florida 32611, USA*
[13]*Louisiana State University, Baton Rouge, Louisiana 70803, USA*
[14]*University of Birmingham, Birmingham, B15 2TT, United Kingdom*
[15a]*INFN, Sezione di Roma, I-00185 Roma, Italy*
[15b]*Università 'La Sapienza', I-00185 Roma, Italy*
[16]*LIGO-Hanford Observatory, Richland, Washington 99352, USA*
[17]*Albert-Einstein-Institut, Max-Planck-Institut für Gravitationsphysik, D-14476 Golm, Germany*
[18]*Montana State University, Bozeman, Montana 59717, USA*
[19]*European Gravitational Observatory (EGO), I-56021 Cascina (PI), Italy*
[20]*Syracuse University, Syracuse, New York 13244, USA*
[21]*University of Western Australia, Crawley, WA 6009, Australia*
[22]*LIGO-Massachusetts Institute of Technology, Cambridge, Massachusetts 02139, USA*
[23]*APC, AstroParticule et Cosmologie, Université Paris Diderot, CNRS/IN2P3, CEA/Irfu, Observatoire de Paris, Sorbonne Paris Cité, 10, rue Alice Domon et Léonie Duquet, 75205 Paris Cedex 13, France*
[24]*Columbia University, New York, New York 10027, USA*
[25a]*INFN, Sezione di Pisa, Italy*
[25b]*Università di Pisa, I-56127 Pisa, Italy*
[25c]*Università di Siena, I-53100 Siena, Italy*
[26]*The University of Texas at Brownsville and Texas Southmost College, Brownsville, Texas 78520, USA*
[27]*San Jose State University, San Jose, California 95192, USA*
[28]*Moscow State University, Moscow, 119992, Russia*
[29a]*LAL, Université Paris-Sud, IN2P3/CNRS, F-91898 Orsay, USA*
[29b]*ESPCI, CNRS, F-75005 Paris, France*
[30]*NASA/Goddard Space Flight Center, Greenbelt, Maryland 20771, USA*
[31]*The Pennsylvania State University, University Park, Pennsylvania 16802, USA*
[32a]*Université Nice-Sophia-Antipolis, CNRS, Observatoire de la Côte d'Azur, F-06304 Nice, France*

[32b]*Institut de Physique de Rennes, CNRS, Université de Rennes 1, 35042 Rennes, France*
[33]*Laboratoire des Matériaux Avancés (LMA), IN2P3/CNRS, F-69622 Villeurbanne, Lyon, France*
[34]*Washington State University, Pullman, Washington 99164, USA*
[35a]*INFN, Sezione di Perugia, Italy*
[35b]*Università di Perugia, I-06123 Perugia, Italy*
[36a]*INFN, Sezione di Firenze, I-50019 Sesto Fiorentino, Italy*
[36b]*Università degli Studi di Urbino 'Carlo Bo', I-61029 Urbino, Italy*
[37]*University of Oregon, Eugene, Oregon 97403, USA*
[38]*Laboratoire Kastler Brossel, ENS, CNRS, UPMC, Université Pierre et Marie Curie, 4 Place Jussieu, F-75005 Paris, France*
[39]*Rutherford Appleton Laboratory, HSIC, Chilton, Didcot, Oxon OX11 0QX United Kingdom*
[40a]*IM-PAN 00-956 Warsaw, Poland*
[40b]*Astronomical Observatory Warsaw University 00-478 Warsaw, Poland*
[40c]*CAMK-PAN 00-716 Warsaw, Poland*
[40d]*Białystok University 15-424 Białystok, Poland*
[40e]*IPJ 05-400 Świerk-Otwock, Poland*
[40f]*Institute of Astronomy 65-265 Zielona Góra, Poland*
[41]*University of Maryland, College Park, Maryland 20742 USA*
[42]*University of Massachusetts-Amherst, Amherst, Massachusetts 01003, USA*
[43]*Canadian Institute for Theoretical Astrophysics, University of Toronto, Toronto, Ontario, M5S 3H8, Canada*
[44]*Tsinghua University, Beijing 100084 China*
[45]*University of Michigan, Ann Arbor, Michigan 48109, USA*
[46]*The University of Mississippi, University, Mississippi 38677, USA*
[47]*Charles Sturt University, Wagga Wagga, NSW 2678, Australia*
[48]*Caltech-CaRT, Pasadena, California 91125, USA*
[49]*INFN, Sezione di Genova, I-16146 Genova, Italy*
[50]*Pusan National University, Busan 609-735, Korea*
[51]*Carleton College, Northfield, Minnesota 55057, USA*
[52]*Australian National University, Canberra, ACT 0200, Australia*
[53]*The University of Melbourne, Parkville, VIC 3010, Australia*
[54]*Cardiff University, Cardiff, CF24 3AA, United Kingdom*
[55a]*INFN, Sezione di Roma Tor Vergata, Italy*
[55b]*Università di Roma Tor Vergata, I-00133 Roma, Italy*
[55c]*Università dell'Aquila, I-67100 L'Aquila, Italy*
[56]*University of Salerno, I-84084 Fisciano (Salerno), Italy and INFN (Sezione di Napoli), Italy*
[57]*The University of Sheffield, Sheffield S10 2TN, United Kingdom*
[58]*RMKI, H-1121 Budapest, Konkoly Thege Miklós út 29-33, Hungary*
[59a]*INFN, Gruppo Collegato di Trento, Italy*
[59b]*Università di Trento, I-38050 Povo, Trento, Italy*
[59c]*INFN, Sezione di Padova, Italy*
[59d]*Università di Padova, I-35131 Padova, Italy*
[60]*Inter-University Centre for Astronomy and Astrophysics, Pune-411, India*
[61]*University of Minnesota, Minneapolis, Minnesota 55455, USA*
[62]*California Institute of Technology, Pasadena, California 91125, USA*
[63]*Northwestern University, Evanston, Illinois 60208, USA*
[64]*The University of Texas at Austin, Austin, Texas 78712, USA*
[65]*Eötvös Loránd University, Budapest, 1117 Hungary*
[66]*University of Adelaide, Adelaide, SA 5005, Australia*
[67]*University of Szeged, 6720 Szeged, Dóm tér 9, Hungary*
[68]*Embry-Riddle Aeronautical University, Prescott, Arizona 86301 USA*
[69]*National Institute for Mathematical Sciences, Daejeon 305-390, Korea*
[70]*Perimeter Institute for Theoretical Physics, Ontario, Canada, N2L 2Y5*
[71]*National Astronomical Observatory of Japan, Tokyo 181-8588, Japan*
[72]*Universitat de les Illes Balears, E-07122 Palma de Mallorca, Spain*
[73]*Korea Institute of Science and Technology Information, Daejeon 305-806, Korea*
[74]*University of Southampton, Southampton, SO17 1BJ, United Kingdom*
[75]*Institute of Applied Physics, Nizhny Novgorod, 603950, Russia*
[76]*Lund Observatory, Box 43, SE-221 00, Lund, Sweden*
[77]*Hanyang University, Seoul 133-791, Korea*
[78]*Seoul National University, Seoul 151-742, Korea*

[79]University of Strathclyde, Glasgow, G1 1XQ, United Kingdom
[80]Southern University and A&M College, Baton Rouge, Louisiana 70813, USA
[81]University of Rochester, Rochester, New York 14627, USA
[82]Rochester Institute of Technology, Rochester, New York 14623, USA
[83]Hobart and William Smith Colleges, Geneva, New York 14456, USA
[84]University of Sannio at Benevento, I-82100 Benevento, Italy and INFN (Sezione di Napoli), Italy
[85]Louisiana Tech University, Ruston, Louisiana 71272, USA
[86]McNeese State University, Lake Charles, Louisiana 70609 USA
[87]University of Washington, Seattle, Washington, 98195-4290, USA
[88]Andrews University, Berrien Springs, Michigan 49104 USA
[89]Trinity University, San Antonio, Texas 78212, USA
[90]Southeastern Louisiana University, Hammond, Louisiana 70402, USA
(Received 16 December 2011; published 19 April 2012)

We report on a search for gravitational waves from coalescing compact binaries using LIGO and Virgo observations between July 7, 2009, and October 20, 2010. We searched for signals from binaries with total mass between 2 and $25M_\odot$; this includes binary neutron stars, binary black holes, and binaries consisting of a black hole and neutron star. The detectors were sensitive to systems up to 40 Mpc distant for binary neutron stars, and further for higher mass systems. No gravitational-wave signals were detected. We report upper limits on the rate of compact binary coalescence as a function of total mass, including the results from previous LIGO and Virgo observations. The cumulative 90% confidence rate upper limits of the binary coalescence of binary neutron star, neutron star-black hole, and binary black hole systems are 1.3×10^{-4}, 3.1×10^{-5}, and 6.4×10^{-6} $\mathrm{Mpc}^{-3}\,\mathrm{yr}^{-1}$, respectively. These upper limits are up to a factor 1.4 lower than previously derived limits. We also report on results from a blind injection challenge.

DOI: 10.1103/PhysRevD.85.082002 PACS numbers: 04.30.Db, 04.80.Cc

I. INTRODUCTION

During 2009 and 2010, both the Laser Interferometer Gravitational-wave Observatory (LIGO) [1] and Virgo [2] gravitational-wave detectors undertook science runs with better sensitivity across a broader range of frequencies than previously achieved. Among the most promising sources of gravitational waves for these detectors are compact stellar mass binaries as they spiral in toward each other and merge. For such systems, which include binary neutron stars (BNS), binary black holes (BBH), and neutron star-black hole binaries (NSBH), the late stages of inspiral and merger occur in the most sensitive band (between 40 and 1000 Hz) of the LIGO and Virgo detectors. In this paper, we report on a search for gravitational waves from binary systems with a maximum total mass of $25M_\odot$, and a minimum component mass of $1M_\odot$.

A hardware injection was performed during the data collection without the knowledge of the data analysis teams as part of a ''blind injection challenge'' [3]. This challenge was intended to test the data analysis procedures and processes for evaluating candidate events. The injection was performed by coherently actuating the mirrors on the LIGO and Virgo detectors to mimic a gravitational-wave signal. Prior to its unveiling as an injection (''unblinding''), the event was determined to be a candidate gravitational wave: it was found to have a false alarm rate of less than 1 in 7000 yr and no evidence for an instrumental or environmental origin could be found. After the analysis of the event was finished it was revealed to be a blind injection and removed from the data.

With the blind injection removed there were no gravitational waves observed above the noise background. As a result we place upper limits on rates of compact binary coalescence (CBC), using upper limits from previous gravitational-wave searches [4] as prior information. The upper limits presented here are up to a factor 1.4 lower than previously derived limits but still 2 to 3 orders of magnitude above expected CBC rates [5].

The paper is laid out as follows. In Sec. II, we provide a brief description of the detectors and their sensitivities during LIGO's sixth science run (S6) and Virgo's second and third science runs. In Sec. III we present a brief overview of the analysis methods used in performing the search. In Sec. IV we discuss the recovery of the blind injection. In Sec. V we present the results of the search with the blind injection removed. In Sec. VI we give the upper limits obtained from the search and close with a brief discussion in Sec. VII.

II. DETECTORS

LIGO comprises two sites, one in Hanford, Washington, and the second in Livingston, Louisiana. The data used in this search were taken during S6, which took place between July 7, 2009, and October 20, 2010. During S6 each of these sites operated a single 4 km laser interferometer, denoted as H1 and L1, respectively. The 2 km H2 instrument at the Hanford site which operated in earlier science runs was not operational in S6. Following LIGO's fifth science run (S5) [1], several hardware changes were made to the LIGO detectors so that prototypes of advanced

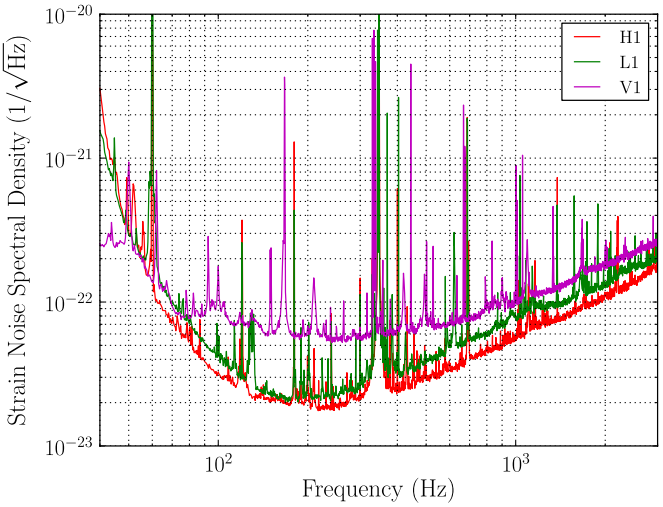

FIG. 1 (color online). Typical detector strain noise spectral density for the LIGO S6 and Virgo VSR2/3 runs. From lowest to highest at 10^2 Hz, the curves are for the H1, L1, and V1 detectors.

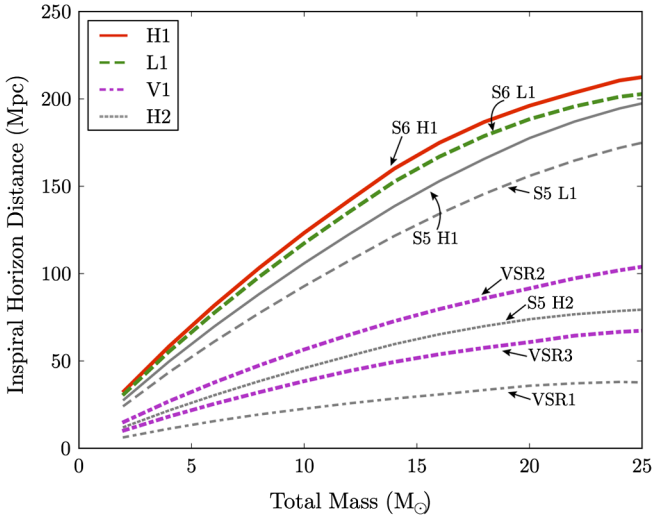

FIG. 2 (color online). Inspiral horizon distance versus the total mass of equal-mass binaries from S5/VSR1 and S6/VSR2/VSR3. The horizon distance is the distance at which an optimally located and oriented binary would produce an expected signal-to-noise ratio of 8. The figure shows the best sensitivity achieved by each detector during the runs.

LIGO technology could be installed and tested [6,7]. This included the installation of a higher power laser, and the implementation of a DC readout system that included a new output mode cleaner on an advanced LIGO seismic isolation table [8]. In addition, the hydraulic seismic isolation system was improved by fine-tuning its feed-forward path.

The Virgo detector (denoted V1) is a single, 3 km laser interferometer located in Cascina, Italy. The data used in this search were taken from both Virgo's second science run (VSR2), which ran from July 7, 2009, to January 8, 2010, and its third science run (VSR3), which ran from August 11, 2010, to October 20, 2010. In the period between the first Virgo science run (VSR1) and VSR2, several enhancements were made to the Virgo detector. Specifically, a more powerful laser was installed in Virgo, along with a thermal compensation system and improved scattered light mitigation. During early 2010, monolithic suspensions were installed, which involved replacing Virgo's test masses with new mirrors hung from fused-silica fibers [9]. VSR3 followed this upgrade.

The sensitivity of the detectors during the S6, VSR2, and VSR3 runs is shown in Fig. 1. The corresponding sensitivity to binary coalescence signals is shown in Fig. 2. This figure shows the distance at which an optimally oriented and located binary would produce a signal-to-noise ratio (SNR) of 8 in a given detector. The figure illustrates the improvement in sensitivity for the LIGO detectors between S5 and S6 and for Virgo between VSR1 and VSR2. The reduction in the horizon distance of the Virgo detector in VSR3 is due to a mirror with an incorrect radius of curvature being installed during the conversion to monolithic suspension.

III. BINARY COALESCENCE SEARCH

To search for gravitational waves from compact binary coalescence [4,10,11], we use matched filtering to correlate the detector's strain output with a theoretical model of the gravitational waveform [12]. Each detector's output is separately correlated against a bank [13] of template waveforms generated at 3.5 post-Newtonian order in the frequency domain [14,15]. Templates were laid out across the mass range such that no more than 3% of the SNR was lost due to the discreteness of the bank. Only nonspinning waveforms with zero eccentricity and a component mass $\geq 1M_\odot$ were generated, and the templates were terminated prior to merger. In the early stages of the run, as in previous searches [4,10,11], the template bank included waveforms from binaries with a total mass $M \leq 35M_\odot$. However, the search results indicated that the higher mass templates ($M > 25M_\odot$) were more susceptible to nonstationary noise in the data. Furthermore, it is at these higher masses where the merger and ringdown phases of the signal come into the detectors' sensitive bands. Consequently, the upper mass limit of this search was reduced to $25M_\odot$ during the latter stages of the science run. Results of a search for higher mass binary black holes using nonspinning, full coalescence (inspiral-merger-ringdown) template waveforms, such as in [16], will be presented in a future publication. Although the template waveforms in this search neglect the spin of the binary components, the search is still capable of detecting binaries whose waveforms are modulated by the effect of spin [17].

We require candidate signals to have a matched-filter SNR greater than 5.5 in at least two detectors, and to have

consistent values of template masses and time of arrival (allowing for travel-time difference) across the detectors where this threshold is exceeded [18]. We use a chi-squared test [19] to suppress non-Gaussian noise transients, which have a high SNR but whose time-frequency evolution is inconsistent with the template waveform. If the reduced chi-squared of a signal, χ_r^2, is greater than unity, we reweight the SNR ρ in order to suppress the significance of false signals, obtaining a reweighted SNR statistic[1]

$$\hat{\rho} = \begin{cases} \frac{\rho}{[(1+(\chi_r^2)^3)/2]^{1/6}} & \text{for } \chi_r^2 > 1, \\ \rho & \text{for } \chi_r^2 \leq 1. \end{cases} \quad (1)$$

Our analysis reports the coalescence time and the quadrature sum, ρ_c, of reweighted SNRs for events coincident between the detectors. The statistic ρ_c is then used to rank events by their significance above the expected background. To measure the background rate of coincident events in the search, we time-shift data from the detectors by an amount greater than the gravitational-wave travel-time difference between detector sites and reanalyze the data. Many independent time-shifts are performed to obtain a good estimate of the probability of accidental coincidence of noise transients at two or more sites.

The background rates of coincident events were initially estimated using 100 time-shifted analyses. These background rates vary depending on the binary's mass—via the waveform duration and frequency band—and also on the detectors involved in the coincidence (the *event type*). The relevant mass parameter is the binary's chirp mass, $\mathcal{M} \equiv (m_1 m_2)^{3/5}(m_1 + m_2)^{-1/5}$, where m_1 and m_2 are the component masses in the binary system. Thus, we sort coincident events into three bins by chirp mass and by event type [10].

The requirement of a coincident signal between at least two sites restricts the times that can be analyzed to four distinct types of *coincident time*. Between July 2009 and October 2010, a total of 0.56 yr of two-or-more-site coincident data was collected. This comprised 0.14 yr of H1L1V1 coincident data, 0.21 yr of H1L1 data, 0.13 yr of H1V1 data, and 0.08 yr of L1V1 data. During H1L1V1 coincident time there are four distinct event types: H1L1V1, H1L1, H1V1, and L1V1. In S6/VSR2, all four event types were kept. In S6/VSR3, H1V1 and L1V1 events in triple-coincident time were discarded due to the heightened rate of transient noise artifacts in Virgo and its decreased sensitivity.

For each candidate, a false alarm rate (FAR) is computed by comparing its ρ_c value to background events in the same mass bin and coincident time and with the same event type. Candidates' FAR values are then compared to background events in *all* bins and event types, over the appropriate coincident time, to calculate a combined FAR. This is the detection statistic which is used to assess the significance of events over the entire analysis time.

Because of the finite number of time-shifts performed, the smallest nonzero FAR that can be calculated is $1/T_{\rm bg}$, where $T_{\rm bg}$ is the total background time obtained by summing the coincident live time in each time-shift. If an event was found to be louder than all background events within its analysis period, additional time-shifted analyses were performed to calculate a more precise FAR for the event.

Although the detectors are enclosed in vacuum systems and isolated from vibrational, acoustic, and electromagnetic disturbances, their typical output data contain a larger number of transient noise events (glitches) with higher amplitude than expected from Gaussian processes alone. Each observatory is equipped with a system of environmental and instrumental monitors that are sensitive to glitch sources but have a negligible sensitivity to gravitational waves. These sensors were used to identify times when the detector output was potentially corrupted [20–23]. We grouped these times into two categories: periods with well-understood couplings between non-gravitational-wave sources and detector output, and periods when a statistical correlation was found but a coupling mechanism was not identified. In our primary search—which included the identification of gravitational-wave candidates and the calculation of upper limits—we removed (*vetoed*) from the analysis times that fell in either of the two categories, along with any coincident events that occurred during these periods. We also performed a secondary search for possible loud candidate events, in which only the times with known couplings were vetoed.

Approximately 10% of the data, designated *playground*, was used for tuning and data quality investigations. These data were searched for gravitational waves, but not used in calculating upper limits. After all vetoes were applied and playground time excluded, there was 0.09 yr of H1L1V1 time, 0.17 yr of H1L1 time, 0.10 yr of H1V1 time, and 0.07 yr of L1V1 time, giving a total analysis time of 0.43 yr.

A substantial change from the analysis procedure of [11] was that data were analyzed in two-week blocks with a latency of two to four weeks, to allow for feedback of information to ongoing detector characterization efforts and to improve data quality. Thus, during the search many new vetoes were introduced resulting from improved understanding of the detectors. However, significant numbers of delta-function-like glitches with large amplitudes remained unvetoed in the LIGO detectors. These were found to cause artifacts in the matched-filter output over a short time surrounding the glitch: thus, during the latter stages of the search, 8 s of time on either side of any matched-filter SNR exceeding 250 was vetoed. Times removed from the primary search by this veto were still examined for possible loud events.

[1]Equation (1) is an improvement over the "effective SNR" used to rank events in [4,10,11]. Most notably, while effective SNR also reweighted SNR using χ_r^2, it became larger than SNR when $\chi_r^2 < 1$. This made it susceptible to overweighting events that had statistical downward fluctuations in χ_r^2.

IV. BLIND INJECTION RECOVERY

The search pipeline described above identified a gravitational-wave candidate occurring on September 16, 2010, at 06:42:23 UTC, with $\rho_c = 12.5$ in coincidence between the two LIGO detectors in the middle mass bin $3.48 \leq \mathcal{M}/M_\odot < 7.40$. The highest matched-filter SNR obtained in the search was 15 at $\mathcal{M} = 4.7M_\odot$ in H1 and 10 at $\mathcal{M} = 4.4M_\odot$ in L1. This difference in SNRs is consistent with typical differences in antenna response factors for these differently oriented detectors. Virgo was also operating at the time of the event, but its sensitivity was a factor of approximately 4 lower than the LIGO detectors; the absence of a signal in Virgo above the single-detector SNR threshold of 5.5 was consistent with this fact. In the LIGO detectors, the signal was louder than all time-shifted H1L1 coincident events in the same mass bin throughout S6. However, with only 100 time-shifts, we could only bound the FAR to $<1/23$ yr, even when folding in all data from the entire analysis. To obtain a better estimate of the event's FAR we performed all possible multiples of 5 sec time-shifts on four calendar months of data around the event, corresponding to an effective analysis time of 2.0×10^5 yr. We found five events with a value of ρ_c equal to or larger than the candidate's, as shown in Fig. 3. These five events were all coincidences between the candidate's signal in H1 and time-shifted transient noise in L1. When we excluded 8 sec from around the event's time in the background estimation, we found *no* background events with ρ_c greater than the candidate and we obtained a significantly different background distribution, also shown in Fig. 3.

Including the events at the time of the candidate in the background estimate, the FAR of the event in the $3.48 \leq \mathcal{M}/M_\odot < 7.40$ mass bin, coincident in the LIGO detectors, was estimated to be 1 in 4×10^4 yr. Since this event occurred in H1L1V1 time during VSR3, only two event types were considered: H1L1 double-coincident events and H1L1V1 triple-coincident events. This resulted in a trials factor of 6 (accounting for the three mass bins and two coincidence types) and a combined FAR of 1 in 7000 yr. The false alarm probability of this event in this analysis, over the 0.47 yr of coincident time remaining after all vetoes were applied, was 7×10^{-5}.

The detectors' environmental monitoring channels record data from seismometers, accelerometers, microphones, magnetometers, radio receivers, weather sensors, and a cosmic ray detector. Injections of environmental signals and other tests indicate that these channels are much more sensitive to environmental signals than the gravitational-wave readout channels are. Arrays of these detectors were operating and providing full coverage at the time of the event, and did not record environmental signals that could account for the event. Environmental signal levels at our observatories and at external electromagnetic weather observatories were typical of quiet times.

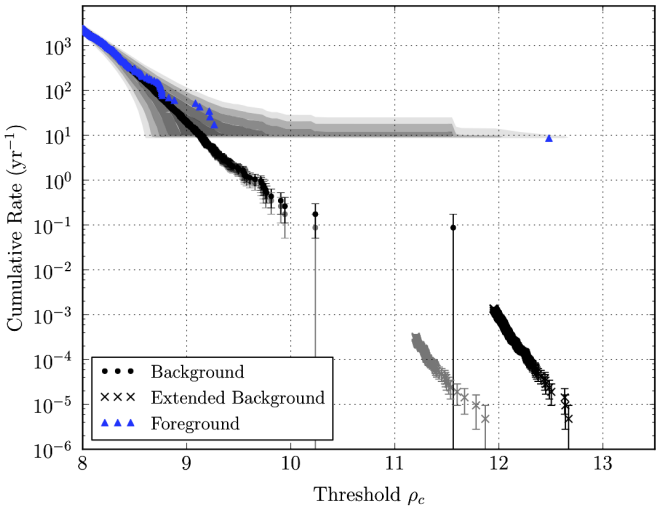

FIG. 3 (color online). The cumulative rate of events with chirp mass $3.48 \leq \mathcal{M}/M_\odot < 7.40$ coincident in the H1 and L1 detectors, seen in four months of data around the September 16 candidate, as a function of the threshold ranking statistic ρ_c. The blue triangles show coincident events. Black dots show the background estimated from 100 time-shifts. Black crosses show the extended background estimation from all possible 5 sec shifts on this data restricted, for computational reasons, to only the tail of loudest events. The gray dots and crosses show the corresponding background estimates when 8 sec of data around the time of the candidate are excluded. Gray shaded contours show the 1-5σ (dark to light) consistency of coincident events with the estimated background including the extended background estimate, for the events and analysis time shown, including the candidate time. This event was later revealed to have been a blind injection.

Mechanisms that could cause coincident signals among widely separated detectors—such as earthquakes, microseismic noise due to large weather systems, and electromagnetic disturbances in the ionosphere [24,25]—were therefore ruled out.

A loud transient occurred in L1 9 sec before the coalescence time of the signal. That transient belonged to a known family of sharp (~ 10 ms) and loud (SNR $\approx$ 200–80 000) glitches that appear 10–30 times per day in the output optical sensing system of this detector. Since the candidate signal swept through the sensitive band of the detector, from 40 Hz to coalescence, in less than 4 sec, it did not overlap the loud transient. Studies, including reanalysis of the data with the glitch removed, indicated that the signal was not related to the earlier instrumental glitch. No evidence was found that the observed signal was associated with, or corrupted by, any instrumental effect.

Following the completion of this analysis, the event was revealed to be a blind injection. While the analysis groups did not know the event was an injection prior to its unblinding, they did know that one or more blind injections may be performed during the analysis period. Such blind injections have been carried out before: see [4] for the

results of a blind injection performed in a previous run. This event was the only coherent CBC blind injection performed during S6 and VSR2 and VSR3. The injection was identified as a gravitational-wave candidate with high probability, and the blind injection challenge was considered to be successful [3].

In order to more accurately determine the parameters of the event prior to the unblinding, we performed coherent Bayesian analyses of the data using models of both spinning and nonspinning compact binary objects [26–30]. These analyses showed evidence for the presence of a weak signal in Virgo, consistent with the signal seen by the two LIGO detectors. The strength of a signal in Virgo is an important input to the localization of a source in the sky. Parameter estimates varied significantly depending on the exact model used for the gravitational waveform, particularly when we included spin effects. However, conservative unions of the confidence intervals from the different waveform models were consistent with most injected parameters, including chirp mass, time of coalescence, and sky location. In addition, the signal was correctly identified as having at least one highly spinning component with the spin misaligned with the angular orbital momentum. We will describe the details of parameter estimation on this and other CBC injections in a future paper.

V. SEARCH RESULTS

After the event was revealed to be a blind injection the data containing it were removed from the analysis. With the injection excluded, there were no gravitational-wave candidates observed in the data. Indeed the search result was consistent with the background estimated from time-shifting the data. The most significant event was an L1V1 coincidence in L1V1 time with a combined FAR of 1.2 yr^{-1}. The second and third most significant events had combined FARs of 2.2 yr^{-1} and 5.6 yr^{-1}, respectively. All of these events were consistent with background: having analyzed $\sim$0.5 yr of data, we would expect the loudest event to have a FAR of 2 ± 2 yr^{-1}. Although no detection candidates were found, a detailed investigation of the loudest events in each analysis period was performed, to improve our understanding of instrumental data quality.

VI. BINARY COALESCENCE RATE LIMITS

Given the absence of gravitational-wave signals, we used our observations to set upper limits on coalescence rates of BNS, BBH, and NSBH systems. We used the procedure described in [31–33] to compute Bayesian 90% confidence level upper limits on the coalescence rate for the various systems, making use of previous results [4,10,11] as prior information on the rates.

The rate of binary coalescences in a spiral galaxy is expected to be proportional to the star formation rate, and hence blue light luminosity, of the galaxy [34]. Previous searches [4,10,11] presented upper limits in terms of blue light luminosity, using units of L_{10}^{-1} yr^{-1}, where one L_{10} is 10^{10} times the solar blue light luminosity. There are, however, numerous challenges to evaluating the upper limit as a function of luminosity, not least due to the large uncertainties in both the luminosity of and distance to nearby galaxies, as well as the lack of a complete galaxy catalogue at larger distances [31,34]. On large scales (greater than $\sim$20 Mpc), the luminosity per unit volume is approximately constant; consequently the analysis can be simplified by reporting upper limits per unit volume per unit time. During the current analysis, the sensitivity of the detectors to the systems of interest (as shown in Fig. 2) was sufficiently large that we could assume signals were uniformly distributed in volume. We therefore quote upper limits in units of $\mathrm{Mpc}^{-3}\,\mathrm{yr}^{-1}$. To incorporate the previous results as prior distributions, we converted from L_{10} to Mpc^3 using a conversion factor of $0.02\mathrm{L}_{10}$ per Mpc^3 [34].

We estimate the volume to which the search is sensitive by reanalyzing the data with the addition of a large number of simulated signals (''software injections'') in order to model the source population. Our ability to detect a signal depends upon the parameters of the source, including the component masses, the distance to the binary, its sky

TABLE I. Rate upper limits of BNS, NSBH, and BBH coalescence, assuming canonical mass distributions. D_{horizon} is the horizon distance averaged over the time of the search. The sensitive distance averaged over all sky locations and binary orientations is $D_{\mathrm{avg}} \simeq D_{\mathrm{horizon}}/2.26$ [35]. The first set of upper limits is those obtained for binaries with nonspinning components. The second set of upper limits is produced using black holes with a spin uniformly distributed between zero and the maximal value of Gm^2/c.

System	BNS	NSBH	BBH
Component masses ($M_\odot$)	1.35/1.35	1.35/5.0	5.0/5.0
D_{horizon} (Mpc)	40	80	90
Nonspinning upper limit ($\mathrm{Mpc}^{-3}\,\mathrm{yr}^{-1}$)	1.3×10^{-4}	3.1×10^{-5}	6.4×10^{-6}
Spinning upper limit ($\mathrm{Mpc}^{-3}\,\mathrm{yr}^{-1}$)	...	3.6×10^{-5}	7.4×10^{-6}

location, and its orientation with respect to the detectors. Numerous signals with randomly chosen parameters were therefore injected into the data. To compute the sensitive volume for a given binary mass, we perform a Monte Carlo integration over the other parameters to obtain the efficiency of the search—determined by the fraction of simulated signals found louder than the loudest foreground event—as a function of distance. Integrating the efficiency as a function of distance then gives the sensitive volume.

We consider several systematic uncertainties that limit the accuracy of the measured search volume and therefore the upper limits [10]: detector calibration errors (conservatively estimated to be 14% in sensitive distance combined over all three detectors and over the entire observational period, and a 2% bias correction), waveform errors (taken to be a one-sided 10% [31] bias toward lower sensitive distance), and Monte Carlo statistical errors (3–5% in sensitive volume). We convert the sensitive distance uncertainties to volume uncertainties, and then marginalize over the uncertainty in volume to obtain an upper limit which takes into account these systematic uncertainties [31].

In Table I we present the marginalized upper limits at the 90% confidence level assuming canonical mass distributions for nonspinning BNS ($m_1 = m_2 = 1.35 \pm 0.04 M_\odot$), BBH ($m_1 = m_2 = 5 \pm 1 M_\odot$), and NSBH ($m_1 = 1.35 \pm 0.04 M_\odot$, $m_2 = 5 \pm 1 M_\odot$) systems. We also compute upper limits as a function of total mass M, using an injection population distributed uniformly over M and uniformly over m_1 for a given M. For NSBH systems we present the upper limit as a function of black hole mass, keeping the neutron-star mass fixed in the range 1–3$M_\odot$. These are presented in Fig. 4. Figure 5 compares the upper limits obtained in this analysis (dark gray regions) to limits obtained in our previous searches up to S5/VSR1 [4] (light gray region) and to astrophysically predicted rates (hatched regions) for BNS, NSBH, and BBH systems. The improvement over the previous limits is up to a factor of 1.4, depending on binary mass; this reflects the additional observation time and improved sensitivity of the S6/VSR2/VSR3 data with respect to all previous observations.

Although we searched with a bank of nonspinning templates, we compute upper limits for NSBH and BBH systems in which one or both of the component masses are spinning. These results are also presented in Table I. We did not compute upper limits for spinning BNS systems because astrophysical observations indicate that neutron stars cannot have large enough spin to significantly affect waveforms observable in the LIGO frequency band [36,37]. Black hole spins were uniformly distributed in both orientation and magnitude, S, with S constrained to the range $0 \leq S \leq Gm^2/c$, and m is the mass of the black hole. As can be seen in Table I, the spinning upper limits are ~16% larger than nonspinning. Signals from spinning systems are recovered with a worse match to our templates since we use a nonspinning template bank.

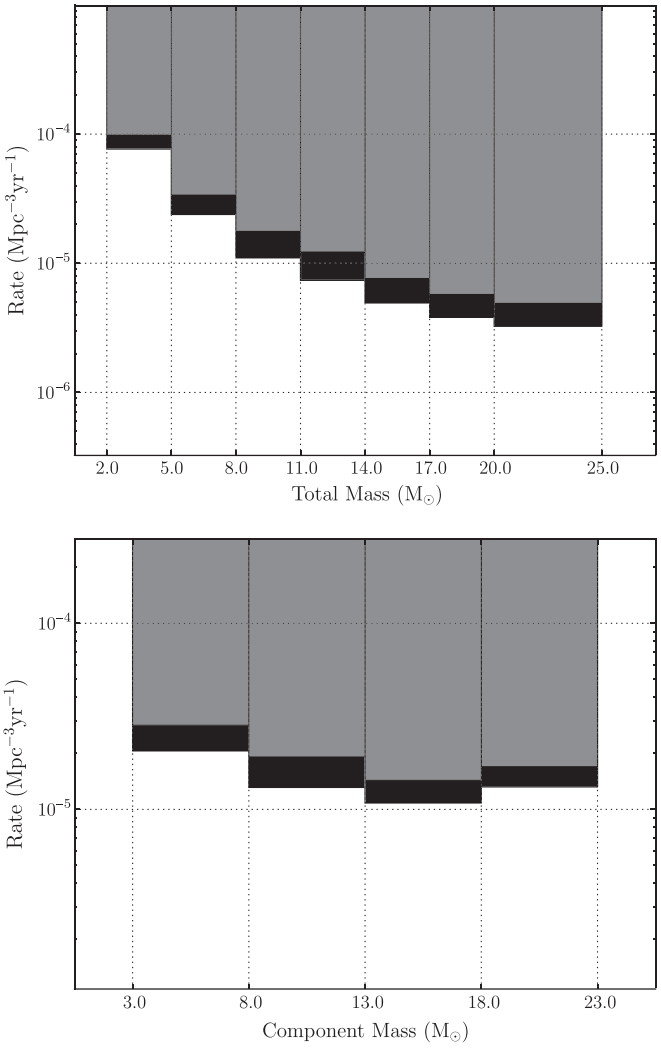

FIG. 4. The marginalized upper limits as a function of mass. The top plot shows the limit as a function of total mass M, using a distribution uniform in m_1 for a given M. The lower plot shows the limit as a function of the black hole mass, with the neutron star mass restricted to the range 1–3$M_\odot$. The light gray bars indicate upper limits from previous searches. The dark bars indicate the combined upper limits including the results of this search.

While the rates presented here represent an improvement over the previously published results from earlier LIGO and Virgo science runs, they are still above the astrophysically predicted rates of binary coalescence. There are numerous uncertainties involved in estimating astrophysical rates, including limited numbers of observations and unknown model parameters; consequently the rate estimates are rather uncertain. For BNS systems the estimated rates vary between 1×10^{-8} and 1×10^{-5} Mpc^{-3} yr^{-1}, with a "realistic" estimate of 1×10^{-6} Mpc^{-3} yr^{-1}. For BBH and NSBH, realistic estimates of the rate are 5×10^{-9} Mpc^{-3} yr^{-1} and 3×10^{-8} Mpc^{-3} yr^{-1} with at least an order of magnitude

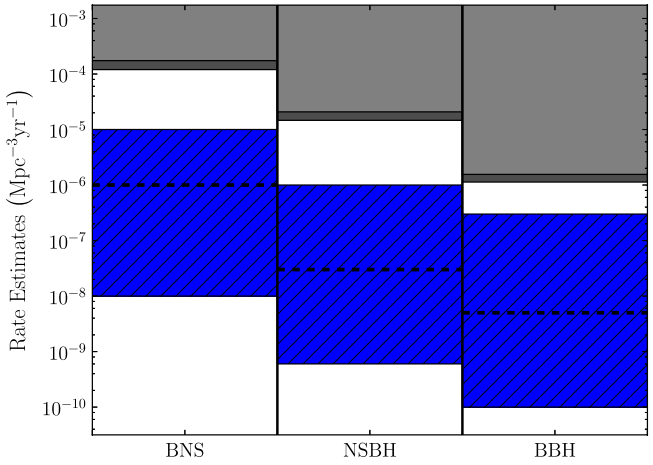

FIG. 5 (color online). Comparison of CBC upper limit rates for BNS, NSBH, and BBH systems. The light gray regions display the upper limits obtained in the S5/VSR1 analysis; dark gray regions show the upper limits obtained in this analysis, using the S5/VSR1 limits as priors. The new limits are up to a factor of 1.4 improvement over the previous results. The lower (blue hatched) regions show the spread in the astrophysically predicted rates, with the dashed-black lines showing the realistic estimates [5]. *Note*: in Ref. [5], NSBH and BBH rates were quoted using a black hole mass of $10M_\odot$. We have therefore rescaled the S5 and S6 NSBH and BBH upper limits in this plot by a factor of $(\mathcal{M}_5/\mathcal{M}_{10})^{5/2}$, where $\mathcal{M}_{10}$ is the chirp mass of a binary in which the black hole mass is $10M_\odot$ and $\mathcal{M}_5$ is the chirp mass of a binary in which the black hole mass is $5M_\odot$.

uncertainty in either direction [5]. In all cases, the upper limits derived here are 2 to 3 orders of magnitude above the realistic estimated rates, and about a factor of 10 above the most optimistic predictions. These results are summarized in Fig. 5.

VII. DISCUSSION

We performed a search for gravitational waves from compact binary coalescences with total mass between 2 and $25M_\odot$ with the LIGO and Virgo detectors using data taken between July 7, 2009, and October 20, 2010. No gravitational waves candidates were detected, and we placed new upper limits on CBC rates. These new limits are up to a factor of 1.4 improvement over those achieved using previous LIGO and Virgo observational runs up to S5/VSR1 [4], but remain 2 to 3 orders of magnitude above the astrophysically predicted rates.

The installation of the advanced LIGO and Virgo detectors has begun. When operational, these detectors will provide a factor of 10 increase in sensitivity over the initial detectors, providing a factor of $\sim$1000 increase in the sensitive volume. At that time, we expect to observe tens of binary coalescences per year [5].

In order to detect this population of gravitational-wave signals, we will have to be able to confidently discriminate it from backgrounds caused by both stationary and transient detector noise. It is customary [5] to assume that a signal with SNR of 8 in each detector would stand far enough above background that we would consider it to be a detection candidate. The blind injection had somewhat larger SNR than 8 in each detector, and we were able estimate a FAR of 1 in 7000 yr for that event. Alternatively, consider a coincident signal with exactly SNR of 8 in two detectors. Provided the signal is a good match to the template waveform ($\chi^2_r \approx 1$ in Eq. (1)) this corresponds to $\rho_c = 11.3$. As can be seen from the extended background events with the blind injection removed in Fig. 3 (light gray crosses), this gives a FAR of $\sim$1 in 2×10^4 yr in a single trial, or 1 in 3000 yr over all trials. Achieving similar-or-better background distributions in Advanced LIGO and Virgo will require detailed data quality studies of the detectors and feedback from the CBC searches, along with well-tuned signal-based vetoes. We have continued to develop the pipeline with these goals in mind. For this analysis we significantly decreased the latency between taking data and producing results, which allowed data quality vetoes to be finely tuned for the CBC search. These successes, along with the successful recovery of the blind injection, give us confidence that we will be able to detect gravitational waves from CBCs at the expected rates in Advanced LIGO and Virgo.

ACKNOWLEDGMENTS

The authors gratefully acknowledge the support of the United States National Science Foundation for the construction and operation of the LIGO Laboratory, the Science and Technology Facilities Council of the United Kingdom, the Max-Planck-Society, and the State of Niedersachsen/Germany for support of the construction and operation of the GEO600 detector, and the Italian Istituto Nazionale di Fisica Nucleare and the French Centre National de la Recherche Scientifique for the construction and operation of the Virgo detector. The authors also gratefully acknowledge the support of the research by these agencies and by the Australian Research Council, the International Science Linkages program of the Commonwealth of Australia, the Council of Scientific and Industrial Research of India, the Istituto Nazionale di Fisica Nucleare of Italy, the Spanish Ministerio de Educación y Ciencia, the Conselleria d'Economia Hisenda i Innovació of the Govern de les Illes Balears, the Foundation for Fundamental Research on Matter supported by the Netherlands Organisation for Scientific Research, the Polish Ministry of Science and Higher Education, the FOCUS Programme of Foundation for Polish Science, the Royal Society, the Scottish Funding Council, the Scottish Universities Physics Alliance, the National Aeronautics and Space Administration, the Carnegie Trust, the Leverhulme Trust, the David and Lucile Packard Foundation, the Research Corporation, and the Alfred P. Sloan Foundation.

[1] B. Abbott *et al.* (LIGO Scientific Collaboration), Rep. Prog. Phys. **72**, 076901 (2009).

[2] F. Acernese *et al.*, Classical Quantum Gravity **25**, 184001 (2008).

[3] LIGO Scientific Collaboration and Virgo Collaboration, The LIGO/Virgo Blind Injection GW100916 (2011), http://www.ligo.org/science/GW100916/.

[4] J. Abadie *et al.* (LIGO Scientific Collaboration and Virgo Collaboration), Phys. Rev. D **82**, 102001 (2010).

[5] J. Abadie *et al.* (LIGO Scientific Collaboration and Virgo Collaboration), Classical Quantum Gravity **27**, 173001 (2010).

[6] R. Adhikari, P. Fritschel, and S. Waldman, Report No. LIGO-T060156-v1, 2006, https://dcc.ligo.org/cgi-bin/DocDB/ShowDocument?docid=7384.

[7] J. Smith, for the LIGO Scientific Collaboration, Classical Quantum Gravity **26**, 114013 (2009).

[8] T. Fricke *et al.*, arXiv:1110.2815 [Classical Quantum Gravity (to be published)].

[9] M. Lorenzini, for the Virgo Collaboration, Classical Quantum Gravity **27**, 084021 (2010).

[10] B. Abbott *et al.* (LIGO Scientific Collaboration), Phys. Rev. D **79**, 122001 (2009).

[11] B. Abbott *et al.* (LIGO Scientific Collaboration), Phys. Rev. D **80**, 047101 (2009).

[12] B. Allen, W. G. Anderson, P. R. Brady, D. A. Brown, and J. D. E. Creighton, arXiv:gr-qc/0509116 [Phys. Rev. D. (to be published)].

[13] S. Babak, R. Balasubramanian, D. Churches, T. Cokelaer, and B. S. Sathyaprakash, Classical Quantum Gravity **23**, 5477 (2006).

[14] L. Blanchet, T. Damour, B. R. Iyer, C. M. Will, and A. G. Wiseman, Phys. Rev. Lett. **74**, 3515 (1995).

[15] L. Blanchet, T. Damour, G. Esposito-Farèse, and B. R. Iyer, Phys. Rev. Lett. **93**, 091101 (2004).

[16] J. Abadie *et al.* (LIGO Scientific Collaboration and Virgo Collaboration), Phys. Rev. D **83**, 122005 (2011).

[17] C. Van Den Broeck *et al.*, Phys. Rev. D **80**, 024009 (2009).

[18] C. A. K. Robinson, B. S. Sathyaprakash, and A. S. Sengupta, Phys. Rev. D **78**, 062002 (2008).

[19] B. Allen, Phys. Rev. D **71**, 062001 (2005).

[20] N. Christensen, for the LIGO Scientific Collaboration and the Virgo Collaboration, Classical Quantum Gravity **27**, 194010 (2010).

[21] F. Robinet, for the LIGO Scientific Collaboration and the Virgo Collaboration, Classical Quantum Gravity **27**, 194012 (2010).

[22] D. M. Macleod, S. Fairhurst, B. Hughey, A. P. Lundgren, L. Pekowsky, J. Rollins, and J. R. Smith, arXiv:1108.0312 [Class. Quant. Grav. (to be published)].

[23] J. Abadie *et al.* (LIGO Scientific Collaboration and Virgo Collaboration), Classical Quantum Gravity (to be published).

[24] N. Christensen, Phys. Rev. D **46**, 5250 (1992).

[25] A. K. Singh and K. Rönnmark, Ann. Geophys. **22**, 2067 (2004).

[26] J. Veitch and A. Vecchio, Phys. Rev. D **81**, 062003 (2010).

[27] F. Feroz, M. P. Hobson, and M. Bridges, Mon. Not. R. Astron. Soc. **398**, 1601 (2009).

[28] M. van der Sluys, V. Raymond, I. Mandel, C. Röver, N. Christensen, V. Kalogera, R. Meyer, and A. Vecchio, Classical Quantum Gravity **25**, 184011 (2008).

[29] M. V. van der Sluys, C. Röver, A. Stroeer, V. Raymond, I. Mandel, N. Christensen, V. Kalogera, R. Meyer, and A. Vecchio, Astrophys. J. **688**, L61 (2008).

[30] C. Röver, Ph.D. thesis, The University of Auckland, 2007, http://hdl.handle.net/2292/2356.

[31] P. R. Brady and S. Fairhurst, Classical Quantum Gravity **25**, 105002 (2008).

[32] P. R. Brady, J. D. E. Creighton, and A. G. Wiseman, Classical Quantum Gravity **21**, S1775 (2004).

[33] R. Biswas, P. R. Brady, J. D. E. Creighton, and S. Fairhurst, Classical Quantum Gravity **26**, 175009 (2009).

[34] R. K. Kopparapu, C. Hanna, V. Kalogera, R. O'Shaughnessy, G. Gonzalez, P. R. Brady, and S. Fairhurst, Astrophys. J. **675**, 1459 (2008).

[35] L. S. Finn and D. F. Chernoff, Phys. Rev. D **47**, 2198 (1993).

[36] R. N. Manchester, G. B. Hobbs, A. Teoh, and M. Hobbs, Astron. J. **129**, 1993 (2005).

[37] T. A. Apostolatos, C. Cutler, G. J. Sussman, and K. S. Thorne, Phys. Rev. D **49**, 6274 (1994).